A Cooperative Compliance Control Framework for Socially Optimal Mixed Traffic Routing

Anni Li, Ting Bai, Yingqing Chen, Christos G. Cassandras and Andreas A. Malikopoulos

Abstract— In this paper, we propose a Cooperative Compliance Control framework for mixed traffic routing, where a Social Planner optimizes vehicle routes for system-wide optimality while a compliance controller incentivizes human drivers to align their behavior with route guidance from the Social Planner through a "refundable toll" scheme. A key challenge arises from the heterogeneous and unknown response models of different human driver types to these tolls, making it difficult to design a proper controller and achieve desired compliance probabilities over the traffic network. To address this challenge, we employ Control Lyapunov Functions to adaptively correct crucial components of our compliance probability model online, construct data-driven feedback controllers, and demonstrate that we can achieve the desired compliance probability for HDVs, thereby contributing to the social optimality of the traffic network.

I. INTRODUCTION

With rapid urbanization and population growth, traffic congestion and safety have long been major concerns for government organizations and society [1], [2]. The Vehicle Routing Problem and its variants have gained significant popularity in research over the past decades [3]. Early approaches relied on static shortest path algorithms, such as Dijkstra's and Floyd-Warshall's algorithms [4]. In a real-world traffic environment, information is always subject to uncertainties, such as actual demand, ongoing user requests, and traffic congestion. These fluctuations have motivated the development of the *dynamic* vehicle routing problem [5], [6], which concurrently integrates real-time traffic data and re-optimizes the routes to adapt to varying conditions in route guidance by utilizing advanced sensing technologies, such as Roadside Units, vehicle-to-vehicle, vehicle-to-infrastructure, and vehicle-to-smart terminal communication [1].

The emergence of Connected and Automated Vehicles (CAVs) has the potential to significantly improve traffic performance and efficiency by better assisting drivers in making decisions to reduce accidents and traffic congestion [7]–[9]. In mixed traffic vehicle routing problems, Human-Driven Vehicles (HDVs) generally operate based on individual driver preferences and limited traffic conditions, leading to *selfish* optimal strategies where each vehicle selects the route that minimizes its own travel cost without considering the broader impact on the network. As a result, this decentralized

decision-making will generally compromise system-wide efficiency and exacerbate traffic congestion [10], [11]. In contrast, *socially* optimal routing aims to minimize the system-wide travel cost by optimizing vehicle routes to balance network utilization and reduce congestion. This approach relies on centralized vehicle coordination, where a Social Planner (SP) collects complete information on the road network and assigns routes that improve the overall efficiency, even if they may not be individually optimal for every vehicle. The implementation of socially optimal routing faces a significant challenge, as HDVs may deviate from assigned routes in pursuit of individual gains [12]–[14].

There has been increasing research focused on integrating social psychology tools and implementing non-monetary management schemes into intelligent transportation systems to improve traffic efficiency and incentivize HDVs to behave in compliant ways. When solving traffic congestion problems, congestion pricing schemes are proposed in [15], [16], where individual drivers have to pay for negative externalities to ensure traffic efficiency. In [17], credit-based congestion pricing is proposed, where drivers receive monetary travel credits to use on roads, while [18] further adopts a mixed economy viewpoint to let eligible users receive travel credits while ineligible users pay out-of-pocket to use the express lanes. To overcome these limitations, non-tradable credit-based congestion pricing schemes have been applied as fair and equitable mechanisms in [19], which proposes a congestion management scheme called "CARMA" utilizing non-tradable "karma credits" for all drivers to bid for the rights to use the express lanes; such credits may be redistributed so that the drivers can choose to benefit themselves now or in the future based on their individual value of time.

In this work, assuming HDVs can communicate with the SP, we propose a *Cooperation Compliance Control* (CCC) framework to incentivize HDVs to comply with the route guidance provided by the SP. The control mechanism is implemented using a *refundable toll* principle, where each vehicle commits a certain number of tokens to a digital wallet at the beginning of its driving period. If the vehicle complies with the reference routes provided by the SP, the committed tokens will be fully refunded. Otherwise, a certain amount of tokens will be removed from the driver's digital wallet. Meanwhile, the SP continuously monitors the real-time system states, updating traffic flow information after a predetermined time window. Consequently, new reference routes will be re-assigned to non-compliant vehicles to mitigate traffic congestion and enhance the overall system-wide traffic efficiency.

A. Li, Y. Chen, and C. G. Cassandras are with the Division of Systems Engineering and Center for Information and Systems Engineering, Boston University, Brookline, MA 02446 (email:{anlianni; yqchenn; cgc}@bu.edu).

T. Bai and A. A. Malikopoulos are with the Information and Decision Science Lab, School of Civil & Environmental Engineering, Cornell University, Ithaca, New York, U.S.A. E-mails: {tingbai, amaliko}@cornell.edu

II. PROBLEM FORMULATION

A. Vehicle Routing Problem

Let $\mathcal{G}(\mathcal{V}, \mathcal{E})$ be the directed graph induced by an urban road network, where $\mathcal{V}$ denotes a set of nodes and $\mathcal{E} \subset \mathcal{V} \times \mathcal{V}$ denotes a set of all edges in the network, and $|\cdot|$ is the cardinality of a set. For any node $i \in \mathcal{V}$ and the directed road edge $e^{ij} \in \mathcal{E}$ from node $i \in \mathcal{V}$ to $j \in \mathcal{V}$, the SP uses a function $s : \mathcal{E} \to \mathbb{R}^+$ as the travel cost for each edge depending on many factors, such as real-time states for other vehicles, road capacity, real traffic flow, travel time, tolls, etc. s^{ij} represents the travel cost for edge $e^{ij} \in \mathcal{E}$.

The vehicle routing problem is essentially identifying the optimal set of routes for a set of vehicles to travel from their origins to their destinations [3]. At any planning time t, let $\mathcal{K}(t) = \{1, 2, ..., N(t)\}$ denote a set that includes all $N(t)$ vehicles in the traffic network. We drop the time t in this section to keep the notation simple. For each vehicle $k \in \mathcal{K}$, its origin and destination nodes are denoted as $O_k, D_k \in \mathcal{V}$, respectively. Let the binary variable $x_k^{ij} \in \{0, 1\}$ denote the optimal route choice from node i to j traversed by vehicle k. Thus, $x_k^{ij} = 1$ means that the edge e^{ij} is included in the optimal route for k. To find the minimal travel cost for the vehicles in the road network, vehicle $k \in \mathcal{K}$ has to satisfy the following constraints.

Flow Balance: The number of times that vehicle $k \in \mathcal{K}$ enters the node $j \in \mathcal{V}/\{O_k, D_k\}$ is equal to the number of times it leaves, i.e.,

$$\sum_{i=1}^{|\mathcal{V}|} x_k^{ij} = \sum_{i=1}^{|\mathcal{V}|} x_k^{ji}, \ \forall j \in \mathcal{V}/\{O_k, D_k\}. \tag{1}$$

Origin and Destination Determination: The vehicle $k \in \mathcal{K}$ leaves its origin O_k and enters the destination D_k are ensured by the following two constraints, respectively:

$$\sum_{j=1}^{|\mathcal{V}|} x_k^{O_k, j} = 1, \ \sum_{i=1}^{|\mathcal{V}|} x_k^{i, D_k} = 1. \tag{2}$$

The constraint (2) ensures that vehicle k starts its trip from O_k and ends at D_k.

Redundant Visit Avoidance: To avoid revisiting the same node in the road network $\mathcal{G}$, each node is limited to be visited at most once, i.e.,

$$\sum_{j=1}^{|\mathcal{V}|} x_k^{ij} \leq 1, \forall i \in \{1, 2, ..., |\mathcal{V}|\}. \tag{3}$$

Sub-tour Elimination: To eliminate sub-tours in the solution, any edge ending at the origin O_k will not be chosen in vehicle k's optimal route(s), and the flow is 0 if the two nodes of an edge are the same, i.e.,

$$\sum_{i=1}^{|\mathcal{V}|} x_k^{i, O_k} = 0, \ x_k^{ii} = 0. \tag{4}$$

B. Social Optimal Guidance

Given a road network modeled as a directed graph $\mathcal{G}(\mathcal{V}, \mathcal{E})$, a SP seeks to enhance its performance by assigning each vehicle k a socially optimal route, denoted as R_k^{ref}. The corresponding travel cost along the edge $e^{ij} \in \mathcal{E}$ is s_k^{ij}, which is time-varying and determined depending on the objective

function of vehicle k and the real traffic conditions. In general, R_k^{ref} can be optimized while improving mobility equity [20] to ensure equity and fairness over all vehicles in the traffic network. Therefore, the travel cost s_k^{ij} may differ across different problem settings. In this paper, we do not specify a particular form for it but instead, keep it in a general form at the discretion of the SP. The SP aims to minimize the travel cost and determines the reference route R_k^{ref} for each vehicle $k \in \mathcal{K}$ by solving the following optimization problem:

$$J_k^{ref} := \min_{x_k^{ij} \in \{0,1\}} \sum_{i=1}^{|\mathcal{V}|} \sum_{j=1}^{|\mathcal{V}|} s_k^{ij} x_k^{ij}, \ \ s.t. \ (1) - (4). \tag{5}$$

Once we obtain the optimal solution x_k^{ij} from the optimization problem (5), the entire reference route R_k^{ref} can be given by $R_k^{ref} = \bigcup_{e^{ij} \in \mathcal{E}} \{e^{ij} \mid x_k^{ij} = 1\}$.

C. Human Preferences

In a mixed-traffic environment, the travel cost s^{ij} on edge e^{ij} designed by the social planner may not be adopted by all HDVs. This divergence occurs because human drivers may either act selfishly by prioritizing only their personal travel time and distance or lack the necessary technology to communicate with other vehicles and access real-time traffic conditions. We define $V_{NC}(t)$, as the set of non-compliant vehicles at time t (for simplicity, we write V_{NC} in the remainder of this subsection), consisting of all HDVs that do not follow the reference trajectory R_k^{ref}, $k \in \mathcal{K}$, their routes are given by the following optimization problem:

$$J_k := \min_{x_k^{ij} \in \{0,1\}} \sum_{i=1}^{|\mathcal{V}|} \sum_{j=1}^{|\mathcal{V}|} c_k^{ij} x_k^{ij}, \ \ s.t. \ (1) - (4). \tag{6}$$

The only difference between the selfish optimal routing problem (6) and the socially optimal routing problem (5) lies in their objectives, where c_k^{ij} denotes the selfish travel cost issued by non-compliant vehicle $k \in V_{NC}$ along the edge e^{ij}. Although we impose no constraints on the choice of c_k^{ij}, the default travel cost for HDVs is generally assumed to be the free flow time, which is commonly provided by widely used navigation tools like Google Maps. Due to the conflict between social and selfish goals, the optimal routes determined by problem (6) may differ from the reference routes given by (5) except for the special case where $c_k^{ij} = s_k^{ij}$.

When non-compliant vehicles deviate from their socially optimal reference routes and choose to travel along the selfishly optimal routes, they may slow down the traffic flow on main roads and lead to congestion. To alleviate such traffic congestion and increase the probability of the non-compliant vehicles complying with the references provided by the SP, a dynamic routing problem is formulated and new references will be provided at their subsequent decision points following any deviation; at the same time, tolls will be deducted from the user's digital wallet to penalize non-compliant behaviors.

III. SOCIAL-COMPLIANCE OPTIMAL PLANNER

In the dynamic routing problem, the travel cost s^{ij} is updated in real time based on the actual traffic conditions monitored by the SP. This update process must account for

the current number of vehicles in the road network while incorporating the effects of newly arriving and exiting vehicle flows. Both the sets $\mathcal{K}(t)$ and $V_{NC}(t)$ are updated each time a vehicle reaches a node and makes a routing decision.

A. Decision Points

In the routing problem, a decision point typically corresponds to an intersection or fork in the road network. Let t_k^m be the time of vehicle k arriving at the m-th decision point along the route from O_k to D_k, and let $d_k^m(t_k^m) \in \mathcal{V}$ denote the actual m-th decision point detected by the SP at time t_k^m. Assuming the cardinality of the set R_k^{ref} is N_k^{ref}, the sequence of nodes along reference route R_k^{ref} at the Origin O_k with time t_k^0 can be written as $\Pi_k^{ref} = \{O_k, d_k^1(t_k^0), d_k^2(t_k^0), ..., d_k^{N_k^{ref}(t_k^0)-1}(t_k^0), D_k\}$.
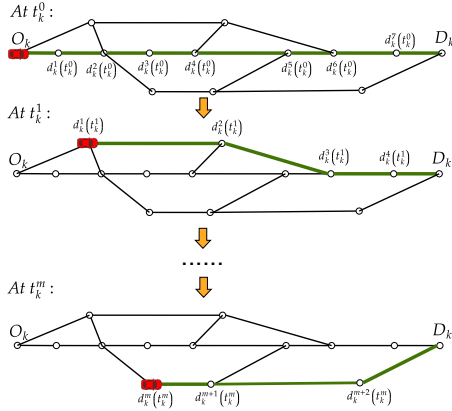

Fig. 1: The order of decision points in a routing problem.

As shown in Fig. 1, each circle is a decision point and the bold green line denotes the updated reference route provided by the SP at each decision point $d_k^m(t_k^m)$. Starting from the origin O_k at time t_k^0, when the non-compliant (red) vehicle $k \in V_{NC}(t_k^0)$ deviates from $\Pi_k^{ref}(t_k^0) := \{O_k, d_k^1(t_k^0), d_k^2(t_k^0), ..., d_k^7(t_k^0), D_k\}$, a new reference route with corresponding nodes $\Pi_k^{ref}(t_k^1) := \{d_k^1(t_k^1), d_k^2(t_k^1), ..., d_k^4(t_k^1), D_k\}$ will be updated by the SP before it arrives at its subsequent decision point $d_k^1(t_k^1)$. By continuously monitoring the actions of a vehicle at decision points, and updating the reference route when a non-compliant vehicle deviates from it, at time t_k^m the nodes of the updated reference route are given by $\Pi_k^{ref}(t_k^m) := \{d_k^m(t_k^m), d_k^{m+1}(t_k^m), ..., D_k\}$, and the actual path up to $d_k^m(t_k^m)$ is defined as $\Pi_k(t_k^m) = \{O_k, d_k^1(t_k^1), d_k^2(t_k^2), ..., d_k^m(t_k^m)\}$.

At each decision point $d_k^m(t_k^m)$, when a deviation of vehicle $k \in V_{NC}(t_k^m)$ is detected by the SP, the node $d_k^m(t_k^m)$ is considered as the new origin and a new reference route can be determined by solving the following optimization problem:

$$J_k^{ref}(t_k^m) := \min_{x_k^{ij}(t_k^m) \in \{0,1\}} \sum_{i=1}^{|\mathcal{V}|} \sum_{j=1}^{|\mathcal{V}|} s_k^{ij}(t_k^m) x_k^{ij}(t_k^m), \, s.t.(1)-(4), \quad (7)$$

where $s_k^{ij}(t_k^m)$ is the travel cost for vehicle k along edge $(i, j) \in \mathcal{E}$ at time t_k^m, and $x_k^{ij}(t_k^m)$ is a binary variable, as in (5), defined at time t_k^m. Essentially, the optimal routing problem (7) is the same as (5) and the only difference is that all the variables in (7) are defined at time t_k^m. Therefore, the

updated reference route at time t_k^m is given by $R_k^{ref}(t_k^m) := \bigcup_{e^{ij} \in \mathcal{E}} \{e^{ij} \mid x_k^{ij}(t_k^m) = 1\}$. Letting $N_k^{ref}(t_k^m)$ denote the cardinality of the set $R_k^{ref}(t_k^m)$, the corresponding sequence of decision points along the reference $R_k^{ref}(t_k^m)$ is given by

$$\Pi_k^{ref}(t_k^m) := (d_k^m(t_k^m), d_k^{m+1}(t_k^m), ..., d_k^{N_k^{ref}(t_k^m)-1}(t_k^m), D_k). \quad (8)$$

B. Compliance Probability

At the m-th decision point $d_k^m(t_k^m)$, a vehicle $k \in V_{NC}(t_k^m)$ has two choices: i) follow the socially optimal reference route $R_k^{ref}(t_k^m)$ assigned by the SP, or ii) adhere to its selfishly optimal routes, given by problem (6), to minimize its own travel costs. Once $\Pi_k^{ref}(t_k^{m-1})$ is provided by the SP at time t_k^{m-1}, the compliant behavior of vehicle k can be measured by checking if the subsequent decision point belongs to the reference route, i.e., whether or not

$$d_k^m(t_k^m) = d_k^m(t_k^{m-1}), \quad (9)$$

where $d_k^m(t_k^{m-1}) \in \Pi_k^{ref}(t_k^{m-1})$. Define a binary variable $\zeta_k(t_k^{m-1})$ to describe the compliance behavior of vehicle k at time t_k^{m-1}:

$$\zeta_k(t_k^{m-1}) = \mathbf{1}[d_k^m(t_k^m) = d_k^m(t_k^{m-1})], \quad (10)$$

where $\mathbf{1}[\cdot]$ is the usual indicator function, i.e., $\zeta_k(t_k^{m-1}) = 1$ when vehicle k is considered compliant at time t_k^{m-1}, otherwise vehicle k is non-compliant at time t_k^{m-1}.

For non-compliant HDVs, we design a cooperative compliance control scheme to incentivize them to align their behaviors with the reference routes through refundable tolls. This is done through a control $u_k(t_k^m)$ that represents the non-compliance cost issued by the SP and applied to the non-compliant vehicle $k \in V_{NC}(t_k^m)$ by deducting an amount $u_k(t_k^m)$ from its digital wallet.

To affect how a human driver k decides to comply or not to the reference route R_k^{ref}, we modify the driver's cost function as follows:

$$J_k^{self}(t_k^m, u_k) = J_k(t_k^m) + \alpha_k(M_k^p(t_k^m) + u_k(t_k^m)), \quad (11)$$

where $J_k(t_k^m)$ denotes the path cost obtained from problem (6). Here, $u_k(t_k^m) > 0$ and is bounded by the "refundable toll" imposed on k at time t_k^0 to prevent $J_k^{self}(t_k^m, u_k)$ from becoming excessively large, while $M_k^p(t_k^m)$ is the accumulated control (digital wallet deductions) over the time interval $[t_k^0, t_k^m]$ determined by $M_k^p(t_k^m) = \sum_{i=1}^{m-1}(1-\zeta_k(t_k^i))u_k(t_k^i)$, where $\zeta_k(t_k^i)$ was defined in (10). Moreover, α_k denotes a weight to measure the importance of the cost controls relative to the selfish path cost evaluated by k. Note that we impose a simple additive control in (11), however, this formulation can be modified to include nonlinear forms, allowing for more flexible and complex strategies.

Remark 1: Even though u_k is positive and bounded, there is still no guarantee that the wallet balance will always remain non-negative. To prevent negative balances, the SP can set specific rules for resetting the digital wallets of such "bad" users, e.g., penalizing them with actual currency, eliminating them from the system or applying restrictions to the access of public infrastructure to incentivize better compliance. ∎

The compliance probability is defined as the likelihood that a vehicle complies with the reference route assigned

by the SP. It is reasonable to assume that for an HDV k, this probability is influenced by the relative difference between the reference route cost and its selfishly optimal route cost as modified in (11) with digital wallet deductions due to non-compliant behavior. Therefore, the value of the compliance probability $P_k(R_k^{ref}(t_k^m))$ satisfies two key properties: $i)$ $P_k(R_k^{ref}(t_k^m))$ decreases as J_k^{ref} increases; and $ii)$ $P_k(R_k^{ref}(t_k^m))$ increases as $u_k(t_k^m)$ (or $M_k^p(t_k^m)$) increases. The exact form of $P_k(R_k^{ref}(t_k^m))$ is obviously unknown and this is complicated by the fact that it is also time-varying. As we will see, this exact form is not crucial as long as the two structural properties above are satisfied so as to capture the driver's trade-off between favoring their selfish route and complying with the socially optimal route. In what follows, we will adopt a form similar to the Boltzmann distribution in [21], and assume that the probability of HDV $k \in V_{NC}(t_k^m)$ following the reference route $R_k^{ref}(t_k^m)$ is given by

$$P_k(R_k^{ref}(t_k^m), u_k) := \frac{e^{-J_k^{ref}(t_k^m)}}{e^{-J_k^{ref}(t_k^m)} + e^{-J_k^{self}(t_k^m, u_k)}}. \quad (12)$$

Here, $J_k^{ref}(t_k^m)$ is the travel cost for vehicle k along reference route $R_k^{ref}(t_k^m)$ at time t_k^m, and $J_k^{self}(t_k^m)$ is the transformed through (11) travel cost for vehicle k along a selfish route, considering both past deducted tokens $M_k^p(t_k^m)$ and the potential future penalty $u_k(t_k^m)$. It is easy to verify that the two properties mentioned above are satisfied by (12).

As already pointed out, in (12) the path costs J_k^{self} and J_k^{ref} are time-varying, as they depend on the actual traffic flow within the road network and the actual position of vehicle k, where the traffic flow is influenced by the behaviors of other non-compliant vehicles. This variation makes it challenging for the SP to effectively design a cooperation compliance control $u_k(t_k^m)$ for each vehicle k at time t_k^m, aiming to increase the compliance probability while avoiding excessive penalties on non-compliant vehicles. In fact, the compliance probability can be viewed as a *state variable* associated with vehicle k that follows unknown dynamics. Given the state measurement and driving it to a desirable value (ideally 1) with unknown dynamics is a task that we pursue next.

C. Cooperation Compliance Control

In this section, we illustrate how to employ CLFs to determine the control $u_k(t_k^m)$, $k \in V_{NC}(t_k^m)$, $m = 0, 1, 2, ...$, to increase the compliance probability in (12) to some desired value Q_k.

In real traffic conditions, it is difficult for the SP to accurately model how humans respond to controls (refundable tolls) in a complex and dynamic environment, making the dynamics of the compliance probability $P_k(R_k^{ref}(t))$ unknown to the SP. Let $\hat{P}_k(t)$ be the estimated compliance probability of vehicle $k \in V_{NC}(t_k^m)$ over time. Then, adopting the general form of an affine system for the dynamics of the estimated compliance probability $\hat{P}_k(t)$, we have

$$\dot{\hat{P}}_k = f_k(\hat{P}_k) + g_k(\hat{P}_k)u_k, \quad (13)$$

where f_k, g_k are Lipschitz continuous functions designed by the SP (based on experience or vehicle driving records),

$u_k \in U$ is the control to vehicle k, and U is the feasible control set, where the lower bound is 0 and the upper bound is determined by the initial value of the digital wallet. The estimated compliance probability dynamics (13) should satisfy the same two properties as (12) to ensure a reliable estimation. This is ensured by restricting $g_k(\cdot)$ to be positive to increase $\hat{P}_k$ as u_k increases, while $f_k(\cdot)$ allows for considerable generality and can be updated at each decision point based on an observed error as defined next, hence exploiting a feedback mechanism.

At each decision point, the error between the estimated compliance probability $\hat{P}_k(t_k^m)$ and our model (12) is

$$e_k(t_k^m) := P_k(R_k^{ref}(t_k^m)) - \hat{P}_k(t_k^m). \quad (14)$$

Thus, the f_k in (13) can be updated by

$$f_k(\hat{P}_k(t_k^m)) = f_k(\hat{P}_k(t_k^{m-1})) + \dot{e}_k(t_k^m). \quad (15)$$

In this way, we always have measurements such that $e_k(t_k^m) = 0$ and $\dot{e}(t_k^m)$ is close to 0 by setting $P_k(R_k^{ref}(t_k^m)) = \hat{P}_k(t_k^m)$. This iteration increases the accuracy of the compliance probability estimation at each decision point.

The SP has two objectives: first, to ensure that the estimated compliance probability $\hat{P}_k(t)$ closely matches $P_k(R_k^{ref}(t))$, and second, to drive the compliance probability $P_k(R_k^{ref}(t))$ toward its desired value Q_k as t increases. To achieve these two objectives, we construct a Lyapunov function for vehicle $k \in \mathcal{K}$ as follows

$$V_k(\hat{P}_k) = \xi_1(\hat{P}_k - Q_k)^2 + \xi_2(\hat{P}_k - P_k(R_k^{ref}))^2, \quad (16)$$

where $\xi_1, \xi_2 \in (0, 1)$ denote weights forming a convex combination above and $Q_k \in [0, 1]$ is a desired compliance probability for vehicle $k \in \mathcal{K}$. We aim for $\hat{P}_k(t_k^m)$ to converge to $P_k(R_k^{ref}(t_k^m))$ and for $\hat{P}_k(t_k^m)$ to converge to Q_k. Once the Lyapunov function (16) is proved to be decreasing and converging to 0, the two objectives of the SP can be achieved, ensuring that the actual compliance probability $P_k(R_k^{ref})$ of vehicle k eventually reaches the desired value Q_k.

Theorem 3.1: (based on [22]) For the system (13), if any locally Lipschitz continuous feedback control law u_k belongs to the set

$$K(\hat{P}_k) = \{u_k \in U : L_f V_k(\hat{P}_k) + L_g V_k(\hat{P}_k)u_k + c_3 V_k(\hat{P}_k) \le 0\} \quad (17)$$

for all $\hat{P}_k$, the Lyapunov function $V_k(\hat{P}_k)$ is an exponentially stabilizing CLF and converges to 0 as $t \to \infty$.

Proof: The set $K(\hat{P}_k)$ consists of the controls that result in $\dot{V}_k(\hat{P}_k) \le -c_3 V_k(\hat{P}_k)$, which further indicates that

$$V_k(\hat{P}_k(t)) \le V_k(\hat{P}_k(t_k^0))e^{-c_3 t}, \quad (18)$$

where $V_k(\hat{P}_k(t_k^0))$ denotes the initial value of the Lyapunov function at time t_k^0. Hence, as proved in [22], for any locally Lipschitz continuous feedback control law u_k such that $u_k \in K(\hat{P}_k)$ for all $\hat{P}_k$, the Lyapunov function $V_k(\hat{P}_k)$ is an exponentially stabilizing Control Lyapunov Function, and converges to 0 as $t \to \infty$. ∎

This result demonstrates that: first, the estimated compliance probability $\hat{P}_k$ converges to its desired value Q_k, and second, $\hat{P}_k$ converges to the actual compliance probability $P_k(R_k^{ref})$. Consequently, this establishes that the actual compliance probability $P_k(R_k^{ref})$ converges to Q_k.

The final step is the determination of the control u_k. Clearly, this has to be selected from the set defined in (17). We proceed in the standard way used to derive controls based on CLFs (see [23]) by updating the control at each decision point $d_k^m(t_k^m)$ as the solution of the following quadratic program:

$$\min_{u_k(t_k^m)\in U, \delta_k(t_k^m)\geq 0} u_k^2(t_k^m) + \gamma\delta_k^2(t_k^m) \tag{19a}$$

$$s.t.\ L_f V_k(\hat{P}_k) + L_g V_k(\hat{P}_k)u_k + c_3 V_k(\hat{P}_k) \leq \delta_k^2, \tag{19b}$$

where δ_k is a controllable variable that relaxes (19b) as a soft constraint, γ is an adjustable weight to capture the relative importance of the two terms in (19a). Note that (19b) relaxes the CLF condition, and it is the one that turns the CLF condition into a soft constraint to ensure the feasibility of the quadratic program (19).

IV. SIMULATION RESULTS

A. Network Setup

We consider a subset of the Boston urban road network, as shown in Fig. 2. The road network consists of 37 nodes and 58 edges, and the length of each edge is labeled in Fig. 2 and is obtained from *GoogleMaps* [24]. The simulation of this network includes 1000 vehicle trips (100 CAVs and 900 HDVs), and their origins and destinations are randomly selected from the red nodes in the road network. The speed limit is set to 35 mph for local road edges and 60 mph for highway edges, and the capacity is 2000 vehicles per hour for each edge. All vehicles are assumed to depart from their origins simultaneously and make decisions at each node (decision point). The real travel time on each edge is modeled by the Bureau of Public Road (BPR) function [25], with parameters $\alpha = 0.14,\ \beta = 4$.
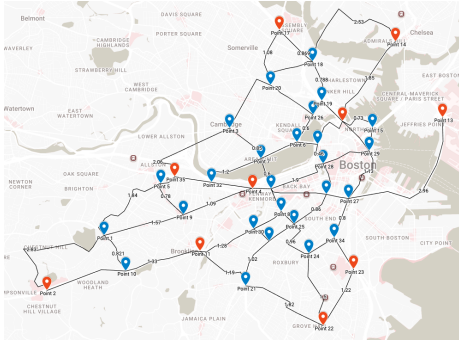

Fig. 2: Boston area road network.

In the simulation, all vehicles are assumed to minimize their travel time for the trip, and all drivers are assumed to restock their digital wallet with actual currency to maintain a positive balance. In problem (7), the travel cost s_k^{ij} is set as the *real flow* time on edge e^{ij}. However, since HDVs lack perfect information about other vehicles in the network, they may estimate their arrival time by using free-flow conditions. The travel cost c_k^{ij} in problem (6) is set as the *free flow* time on edge e^{ij}. This discrepancy can lead to traffic congestion and reduce the overall efficiency of the network.

B. Results and Analysis

At each decision point $d_k^m(t_k^m)$, the SP updates the travel cost $s_k^{ij}(t_k^m)$ for all edges $e^{ij} \in \mathcal{E}$ based on real-time traffic flow information. New reference routes are then reassigned to all vehicles after detecting non-compliant behaviors to minimize traffic disruptions. The time window for estimating the real traffic flow is $\Delta t = 120s$. In (11), the parameter is set as $\alpha_k = 3$, and the dynamics of the estimated compliance probability in (13) are given by $\dot{\hat{P}}_k = f_k(\hat{P}_k(t_k^m)) + u_k$, where $f_k(\hat{P}_k(0)) = 0$ and will be updated at each t_k^m, and we have set $g_k(t) = 1$ for all t. The weights in (16) are set as $\xi_1 = 0.5, \xi_2 = 0.5$ to balance the estimation error and desired value reachability. In (19), the parameters are $\gamma = 0.5$, $c_3 = 100$. The desired compliance probability is set as $Q^* = 0.9$ with $Q_k = 0.9,\ \forall k \in \mathcal{K}$.
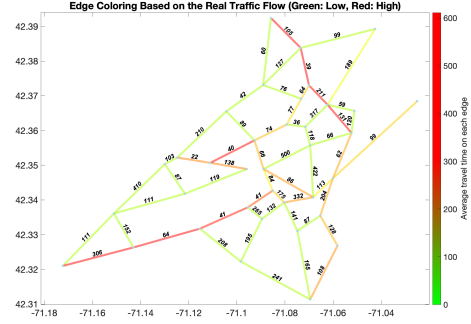
(a) Average travel time of each edge under Baseline.
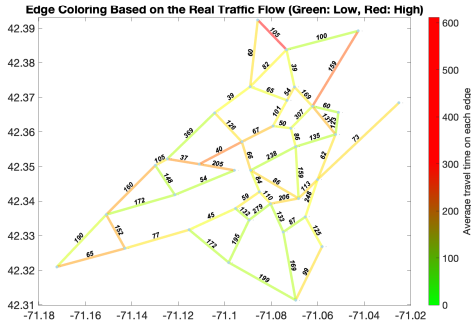
(b) Average travel time of each edge under CCC.

Fig. 3: Average travel time of each edge.

We consider the selfish optimal planning problem given by (6) as the "Baseline". The average travel time per vehicle decreased from 1342.9s in the Baseline case to 1003.9s in the socially optimal case after the SP applied control $u_k(t_k^m)$ at each decision point where a vehicle deviates from the SP reference route, representing a 25.2% reduction. After implementing the CCC framework, the maximum and minimum travel times are reduced to $1340.1s$ and $581.9s$, respectively, compared to $2129.7s$ and $805.6s$ in Baseline.

Additionally, the traffic congestion, which is captured by the average travel time along each edge, is illustrated in Fig. 3(a) for Baseline and in Fig. 3(b) for CCC. In these two figures, green edges represent travel times at or below the free-flow level, red edges exceed twice the free-flow time, and orange edges fall in between. In Fig. 3(a), there are 8 red edges and some green edges, indicating that some parts of the network are heavily congested while others

remain underutilized. However, in Fig. 3(b), when the SP assigns socially optimal reference routes to each vehicle and implements CCC to address non-compliant behaviors, the network utilization increases. As a result, there are no red edges and no heavy traffic congestion, indicating that the traffic distribution across the map is more balanced.

The evolution of the compliance probability as a function of the number of decision points is illustrated in Fig. 4. At each decision point, the control u_k for vehicle k is updated, leading to a corresponding update in $P_k(R_k^{ref})$. Note that vehicles reach decision points at different times in the routing problem, causing compliance probability updates to occur *asynchronously* across different vehicles. As shown in Fig. 4, the compliance probability has increased from 0 to approximately 0.9 for all vehicles after passing 5 decision points, demonstrating the effectiveness of the cooperative compliance control in (19). This result confirms that the actual compliance probability can converge to the desired value, even when its dynamics are unknown to the SP.

Note that the convergence of the compliance probability is not required to be achieved within a single trip. The desired value Q_k can be reached either within a single trip or over multiple trips, depending on the path length and the number of decision points encountered along the path. After each trip, the driver starts the next trip with the latest digital wallet balance and re-initializes the compliance probability based on (12), causing the convergence process to evolve over a long-term horizon.
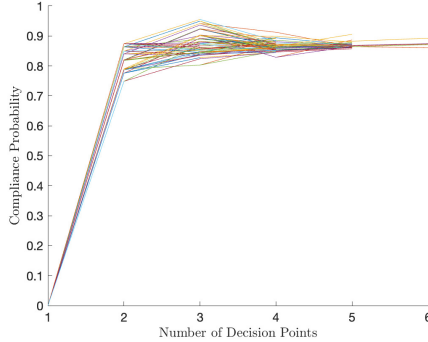

Fig. 4: Compliance Probability Convergence.

V. CONCLUSIONS AND FUTURE WORK

In this paper, we presented a CCC framework designed for mixed traffic routing problems, aimed at incentivizing non-cooperative HDVs to adhere to the system-wide optimal route guidance established by a SP through a refundable toll scheme. To address the heterogeneous and unpredictable dynamics of human driver responses, we employed CLFs, enabling us to adaptively update our compliance probability model online and ensure the convergence of actual compliance probabilities to desired values, thereby enhancing the efficiency of the road network. The results of our simulations demonstrated the CCC framework's effectiveness in reducing travel times for vehicle trips and alleviating traffic congestion. Future research will explore the application of advanced machine-learning techniques to accurately model human compliance probabilities based on historical data.

REFERENCES

[1] M. Jeihani, A. Ansariyar, E. Sadeghvaziri, A. Ardeshiri, M. M. Kabir, A. Haghani, A. Jones, E. Center *et al.*, "Investigating the effect of connected vehicles (CV) route guidance on mobility and equity," 2022.

[2] M. van Essen, O. Eikenbroek, T. Thomas, and E. van Berkum, "Travelers' compliance with social routing advice: Impacts on road network performance and equity," *IEEE transactions on intelligent transportation systems*, vol. 21, no. 3, pp. 1180–1190, 2019.

[3] P. Toth and D. Vigo, *The vehicle routing problem*. SIAM, 2002.

[4] P. Höfner and B. Möller, "Dijkstra, floyd and warshall meet kleene," *Formal Aspects of Computing*, vol. 24, pp. 459–476, 2012.

[5] L. Abbatecola, M. P. Fanti, and W. Ukovich, "A review of new approaches for dynamic vehicle routing problem," in *2016 IEEE International Conference on Automation Science and Engineering (CASE)*. IEEE, 2016, pp. 361–366.

[6] U. Ritzinger, J. Puchinger, and R. F. Hartl, "A survey on dynamic and stochastic vehicle routing problems," *International Journal of Production Research*, vol. 54, no. 1, pp. 215–231, 2016.

[7] A. A. Malikopoulos, L. E. Beaver, and I. V. Chremos, "Optimal time trajectory and coordination for connected and automated vehicles," *Automatica*, vol. 125, no. 109469, 2021.

[8] W. Xiao and C. G. Cassandras, "Decentralized optimal merging control for connected and automated vehicles with safety constraint guarantees," *Automatica*, vol. 123, p. 109333, 2021.

[9] A. Li, A. S. C. Armijos, and C. G. Cassandras, "Robust optimal lane-changing control for connected autonomous vehicles in mixed traffic," *Automatica*, vol. 174, p. 112169, 2025.

[10] T. Roughgarden, *Selfish routing and the price of anarchy*, 2005.

[11] R. Feldmann, M. Gairing, T. Lücking, B. Monien, and M. Rode, "Selfish routing in non-cooperative networks: A survey," in *Mathematical Foundations of Computer Science 2003: 28th International Symposium, MFCS 2003, Bratislava, Slovakia, August 25-29, 2003. Proceedings 28*. Springer, 2003, pp. 21–45.

[12] A. Li and C. G. Cassandras, "Towards achieving cooperation compliance of human drivers in mixed traffic," *2025 American Control Conference (to appear) arXiv:2405.17594*, 2024.

[13] P.-A. Chen and D. Kempe, "Altruism, selfishness, and spite in traffic routing," in *Proceedings of the 9th ACM Conference on Electronic Commerce*, 2008, pp. 140–149.

[14] A. Sadeghi, F. Aros-Vera, H. Mosadegh, and R. YounesSinaki, "Social cost-vehicle routing problem and its application to the delivery of water in post-disaster humanitarian logistics," *Transportation research part E: logistics and transportation review*, vol. 176, p. 103189, 2023.

[15] A. Pigou, *The economics of welfare*. Routledge, 2017.

[16] A. De Palma and R. Lindsey, "Traffic congestion pricing methodologies and technologies," *Transportation Research Part C: Emerging Technologies*, vol. 19, no. 6, pp. 1377–1399, 2011.

[17] K. M. Kockelman and S. Kalmanje, "Credit-based congestion pricing: a policy proposal and the public's response," *Transportation Research Part A: Policy and Practice*, vol. 39, no. 7-9, pp. 671–690, 2005.

[18] D. Jalota, J. Lazarus, A. Bayen, and M. Pavone, "Credit-based congestion pricing: Equilibrium properties and optimal scheme design," in *2023 62nd IEEE Conference on Decision and Control (CDC)*. IEEE, 2023, pp. 4124–4129.

[19] E. Elokda, C. Cenedese, K. Zhang, J. Lygeros, and F. Dörfler, "CARMA: Fair and efficient bottleneck congestion management with karma," *arXiv preprint arXiv:2208.07113*, 2022.

[20] T. Bai, A. Li, G. Xu, C. G. Cassandras, and A. A. Malikopoulos, "Routing guidance for emerging transportation systems with improved dynamic trip equity," *arXiv:2503.12601*, 2025.

[21] J. Rowlinson*, "The Maxwell–Boltzmann distribution," *Molecular Physics*, vol. 103, no. 21-23, pp. 2821–2828, 2005.

[22] A. D. Ames, K. Galloway, K. Sreenath, and J. W. Grizzle, "Rapidly exponentially stabilizing Control Lyapunov Functions and hybrid zero dynamics," *IEEE Transactions on Automatic Control*, vol. 59, no. 4, pp. 876–891, 2014.

[23] W. Xiao, C. G. Cassandras, and C. Belta, *Safe Autonomy with Control Barrier Functions: Theory and Applications*. Springer Nature, 2023.

[24] GoogleMaps, *https://www.google.com/maps*.

[25] U. S. B. of Public Roads, *Traffic Assignment Manual for Application with A Large, High Speed Computer*. US Department of Commerce, Bureau of Public Roads, Office of Planning, Urban, 1964, vol. 37.